Non-esterified free fatty acids (NEFA) enhance the inflammatory response in renal tubules by inducing extracellular ATP release

Hong Sun[1,2], Ziling Sun[2], Zac Varghese[3], Yinfeng Guo[2], John F. Moorhead[3], Robert J. Unwin[3] and Xiong Z. Ruan[3,4]

1. Department of Endocrinology and Metabolism, the First Affiliated Hospital of Soochow University, Suzhou 215123, China.
2. Department of Endocrinology and Metabolism, Zhongda Hospital, Institute of Diabetes, Medical School, Southeast University, Nanjing 210009, China.
3. John Moorhead Research Laboratory, Department of Renal Medicine, University College London (UCL) Medical School, Royal Free Campus, London, NW3 2PF, UK.
4. Centre for Lipid Research & Key Laboratory of Molecular Biology for Infectious Diseases (Ministry of Education), Institute for Viral Hepatitis, Department of Infectious Diseases, the Second Affiliated Hospital, Chongqing Medical University, Chongqing, PR. China, 400016.

Correspondence to Dr Xiong Z. Ruan, John Moorhead Research Laboratory, Department of Renal Medicine, University College London, Rowland Hill Street, London NW3 2PF, UK. E-mail: x.ruan@ucl.ac.uk

Running head: Fatty acids cause extracellular ATP release

Abstract

In proteinuric renal diseases, excessive plasma non-esterified free fatty acids (NEFA) bound to albumin can leak across damaged glomeruli to be reabsorbed by renal proximal tubular cells and cause inflammatory tubular cells damage by as yet unknown mechanisms. The present study was designed to investigate these mechanisms induced by palmitic acid (PA, one of NEFA) overload. Our results show that excess PA stimulates ATP release through the pannexin1 (Panx1) channel in human renal tubule epithelial cells (HK-2); increasing extracellular ATP (eATP) concentration approximately three-fold in comparison with control. The ATP release is dependent on caspase-3/7 activation induced by mitochondrial reactive oxygen species (mtROS). Furthermore, eATP aggravates PA-induced monocyte chemoattractant protein-1 (MCP-1) secretion and monocyte infiltration of tubular cells, enlarging the inflammatory response in both macrophages and HK-2 cells via the purinergic P2X7 receptor (P2X7R)-mTOR-FOXO1-TXNIP/NLRP3 inflammasome pathway. Hence, PA increases mtROS-induced ATP release and inflammatory stress, which cause a 'first hit', while ATP itself is a 'second hit' in amplifying the renal tubular inflammatory response; thus, inhibition of ATP release or P2X7R may be an approach to reduce renal inflammation and improve renal function.

Keywords: non-esterified free fatty acids, ATP, the P2X7R-mTOR-FOXO1-TXNIP/NLRP3 inflammasome pathway, renal tubular inflammation

Abbreviations: CKD, chronic kidney disease; NEFA, non-esterified free fatty acids; PA, palmitic acid; Panx1, pannexin1; mtROS, mitochondrial reactive oxygen species; eATP, extracellular ATP; IL-1β, interleukin-1β; P2X7R, purinergic P2X7 receptor; Tm, tunicamycin; MT, Mito-TEMPO; MCP-1, monocyte chemoattractant protein-1; TXNIP, thioredoxin-interacting protein; FOXO1, forkhead boxO1; mTOR,

mammalian target of rapamycin; HK-2, human renal tubule epithelial cell line; THP-1, human monocyte cell line.

Introduction

Chronic kidney disease (CKD) is a major global health problem. The severity of tubulointerstitial inflammation has long been considered as a crucial determinant of progressive CKD (19, 29). Although the pathogenesis of tubulointerstitial inflammation is poorly understood, proteinuria is one common association and likely to be a pathogenic factor (16). It is known that the uptake of albumin is mediated by the megalin-cubilin complex and also by CD36 in renal proximal tubules (3, 7). However, the effect of albumin-bound plasma non-esterified free fatty acids (NEFA) on these uptake mechanisms remains unclear.

Albumin normally carries >99% of plasma NEFA (36). In nephrosis, the NEFA load per albumin molecule is markedly increased. NEFA bound to albumin are filtered through the glomeruli and reabsorbed by the proximal tubular cells and may mediate tubular damage in proteinuric renal disease (35). Several experimental studies have shown that an excessive NEFA load in proteinuria induces severe tubulointerstitial injury, consisting of inflammatory cell infiltration, renal tubular cell apoptosis, and oxidative stress (21, 33); however, the underlying mechanisms are still unknown.

Recent studies have demonstrated that NEFA can stimulate ATP release from liver cells, which has been suggested as a causative factor in human nonalcoholic steatohepatitis (38). Furthermore, evidence shows that the release of ATP under physiological and pathophysiological conditions can be mediated by an integral membrane protein known as pannexin 1 (Panx1) (5), which is present in many cell types, including renal tubular cells (8). However, whether NEFA can cause ATP release via Panx1 channels in renal tubular cells is unknown. Panx1 can be activated during apoptosis by direct caspase-3/7 cleavage of its C-terminus, resulting in removal of the last 45–50 amino acids; Panx1 then forms a channel that is capable of

allowing permeation of relatively large molecules, including ATP (5, 12). Since a variety of toxic stimuli can cause production of mitochondrial reactive oxygen species (mtROS) that may trigger mitochondrial apoptotic signaling pathways (22, 34), caspase-3/7 could be activated by NEFA-induced mtROS production, leading to Panx1 channel opening and ATP release from renal tubular cells.

Studies have shown that high (supra-micromolar) local concentrations of extracellular ATP (eATP) can mediate sustained activation of the purinergic P2X7 receptor (P2X7R), resulting in the secretion of interleukin-1β (IL-1β) (13). Furthermore, a growing body of evidence supports a causative role for IL-1β in the pathogenesis of renal tubulointerstitial inflammation, kidney injury, and CKD. The processing and production of IL-1β require two signals: the first induces transcription and translation of pro-IL-1β, and the second activation of the NLRP3 inflammasome (comprising the NOD-like receptor protein 3, the adapter ASC, and pro-caspase-1) to cause the autocatalytic cleavage of pro-caspase-1 to caspase-1. Subsequently, the activated caspase-1 cleaves the inactive precursor of the IL-1β to its biologically active form. The cytoplasmic thioredoxin-interacting protein (TXNIP) is a known binding partner for NLRP3 and is necessary for downstream inflammasome formation and activation (1, 24, 41). The transcription factor forkhead boxO1 (FOXO1) regulates many cellular processes, including cell cycle progression, cell death, differentiation, stress resistance, and metabolism (26, 28), and has been shown to control TXNIP expression (20, 25, 39). Moreover, FOXO1 is downstream of the mammalian target of rapamycin (mTOR) signaling pathway; when phosphorylated, mTOR (p-mTOR) suppresses FOXO1 transcriptional activity (6, 18), which may in turn affect TXNIP expression and thereby the inflammasome response. Since the blockade of P2X7R can suppress mTOR phosphorylation (4), we hypothesise that eATP-P2X7R may upregulate FOXO1, which enhances the transcription and translation of TXNIP, followed by activation of the NLRP3 inflammasome, and ultimately, causing the cleavage and release of IL-1β.

Accordingly, we propose that in renal tubular cells, an NEFA-induced increase in mtROS production and inflammatory stress cause a 'first hit' that stimulates ATP release via the Panx1 channel activated by caspase-3/7, followed by an increase in extracellular ATP (eATP) that mediates the 'second hit' through P2X7R stimulation, inflammasome activation and inflammatory response, involving the inhibition of mTOR and the upregulation of FOXO1and TXNIP.

Materials and methods

Cell culture

A human renal tubule epithelial cell line (HK-2) and a human monocyte cell line (THP-1) were obtained from the American Type Culture Collection (Manassas, VA, USA). HK-2 and THP-1 cells were cultured in RPMI 1640 (Lonza, Slough, UK) containing 10% fetal calf serum, 2mM L-glutamine solution, 100 U/ml penicillin and 100 μg/ml streptomycin (Sigma, Dorset, UK). THP-1 cells were differentiated into macrophages after being triggered with 160 nM phorbol-12-myristate-13-acetate (PMA, Sigma) for 72 h, and the differentiated THP-1 macrophages were washed extensively with phosphate-buffered saline (PBS, Gibco, Paisley, UK) before use. All experiments were performed in serum-free RPMI 1640 medium containing 0.2% BSA (Sigma). Palmitic acid (PA, conjugated with albumin), ATP, A438079 (a selective P2X7R antagonist) and tunicamycin (Tm, an N-linked glycosylation inhibitor) were purchased from Sigma. Mito-TEMPO (MT, a mitochondria-targeted antioxidant) was obtained from Santa Cruz Biotechnology (Wiltshire, UK).

mtROS production

mtROS production was determined using dihydroethidium (Thermo Fisher Scientific, Dartford, UK) according to the manufacturer's instructions. In brief, 1×10^4 HK-2 cells/well were seeded in an 8-well chamber slide (Becton Dickinson, Oxford, UK) and incubated in a serum-free experimental medium in the absence or presence of 3.2mM PA, PA plus 10uM MT, or MT alone. After 24 h incubation, the cells were cultured in medium containing 5μM of dihydroethidium at 37 °C for 30 min; then the

medium was removed; the cells washed three times with PBS and observed under a fluorescence microscope (Carl Zeiss, Hertfordshire, UK).

Measurement of ATP release

HK-2 cells were seeded in a 6-well plate. After a 24 h starvation period, the cells were treated under different experimental conditions as described above. 24 h later, culture supernatants were collected, and the supernatant ATP was detected by an ATP Assay Kit (Abcam, Cambridge, UK) according to the manufacturer's instructions. In brief, a standard curve dilution was prepared and the samples deproteinized. Then, the reaction mix was added and the samples incubated for 30 min at room temperature. The absorbance was determined at 570 nm using a microplate reader. Concentration of samples in the test samples is calculated as: [ATP] (nmol per ul or mM) = (Ts/Sv) × D [Ts = ATP amount from standard curve (nmol or mM); Sv = sample volume added in sample wells (µl); D = sample dilution factor.].

Caspase-3/7 activity

Caspase-3/7 activity was determined by CellEvent™ Caspase-3/7 Green ReadyProbes® Reagent (Thermo Fisher Scientific) according to the manufacturer's instructions. In brief, 1×10^4 HK-2 cells/well were seeded in an 8-well chamber slide and incubated in different serum-free experimental conditions for 24 h. After 2 drops/ml of reagent had been added into the medium, cells were incubated for 1 h at room temperature. Then, the medium was removed; the cells washed three times with PBS and observed under a fluorescence microscope (Carl Zeiss).

YoPro-1 uptake

YoPro-1 has a molecular mass of ~600 Da (similar to ATP) and does not permeate biological membranes. YoPro-1 is not fluorescent in solution, but becomes fluorescent on binding to nucleic acids. Panx1 activation stimulates YoPro-1 uptake, and YoPro-1 fluorescence has been used to quantify Panx1 activation (5, 37). For these experiments, HK-2 cells were seeded in an 8-well chamber slide and incubated in different serum-free experimental conditions. After a 24 h incubation, the cells were cultured in medium containing 5µM YoPro-1 Iodide (Thermo Fisher Scientific) at 37 °C for 30

min. The medium was then removed and the cells washed three times with PBS and observed under a fluorescence microscope (Carl Zeiss).

Transwell filter migration assay and enzyme-linked immuno sorbent assay (ELISA)

HK-2 cells were seeded in a 6-well plate and treated with the experimental medium in the absence or presence of 3mM eATP, 3.2mM PA or eATP plus PA. After a 24 h incubation, culture supernatants were harvested. Microporous membrane (pore size 8 μm) transwell inserts (Millipore, Watford, UK) were used for the chemotaxis assay. THP-1 cells in 200μl serum-free RPMI were added to the upper chamber, with 500μl above culture supernatants in the lower chamber. THP-1 cells were allowed to migrate for 2 h incubation at 37 °C，5 % CO_2，and then the inserts were fixed and stained with crystal violet (Sigma). The non-migratory cells were removed before the membrane was mounted and the number of migratory cells was observed under a microscope (Carl Zeiss). The monocyte chemoattractant protein-1 (MCP-1) in the supernatants was detected by MCP-1 ELISA kit (Abcam) according to the manufacturer's instructions.

RNA extraction and real-time PCR

Total RNA was isolated from cultured THP-1 macrophages or HK-2 cells using TRIzol (Ambion, Huntingdon, UK). Then, RNA (1μg) was used as a template for RT with a High Capacity cDNA RT Kit from ABI (Applied Biosystems, Warrington, UK). Real-time RT-PCR was performed on an ABI 7000 Sequence Detection System using SYBR Green dye according to the manufacturer's protocol (Applied Biosystems). All PCR primers were synthesized by Sigma. The sequences and the amplified lengths are shown in Table 1.

Protein extraction and western blot analysis

Proteins from whole-cell extract and supernatant were denatured and then subjected to electrophoresis on 6%~15% SDS polyacrylamide gels. Polyvinylidene fluoride

membrane (GE Healthcare, Buckinghamshire, UK) was used for transfer and then blocked for 1 h at room temperature with 5% bovine serum albumin in Tris-buffered saline containing 0.05% Tween 20 (TBST). Subsequently, blots were washed and incubated overnight at 4 °C in TBST containing 5% bovine serum albumin with the following antibodies: rabbit anti-human IL-1β antibody (Abcam), rabbit anti-human caspase-1 antibody (Santa Cruz Biotechnology), rabbit anti-human TXNIP (Invitrogen, Paisley, UK), rabbit anti-human FOXO1 (Abcam), rabbit anti-human phosphorylated mTOR (p-mTOR) antibody (Abcam) and β-actin antibody (Thermo Fisher Scientific). Membranes were washed three times with TBST, incubated with goat anti-rabbit horseradish peroxidase-labeled antibody (Abcam) in antibody dilution buffer for 1h at room temperature and then washed three times with TBST. Finally, detection procedures were performed using an ECL Advance Western blotting detection kit and autoradiography was performed on Hyperfilm ECL (Amersham Bioscience, Buckinghamshire, UK). For quantitative analysis, bands were detected and evaluated densitometrically with LabWorks software (UVP Laboratory Products, USA) and normalised for β-actin density.

Statistics

All data were analyzed using the SPSS software version 20.0. The normal distribution of the data was checked by the Kolmogorov-Smirnov test. Normally distributed data were expressed as mean ± SEM and multiple comparissons were made using one-way analysis of variance (ANOVA) followed by Bonferroni's multiple comparison tests. Differences were considered significant when P values < 0.05.

Results

PA induced ATP release from renal tubular cells in a mtROS-dependent way

To assess whether NEFA stimulated mtROS production in renal tubular cells, HK-2 cells were treated with PA for 24 h. Results showed that PA significantly increased

mtROS production, which could be inhibited by MT, a mitochondria-targeted antioxidant (Fig.1A). In addition, PA stimulated ATP release from the cells by showing a 3-fold increase of eATP concentration compared with control; MT reduced the release of ATP in PA-treated HK-2 cells. MT alone had no effect on ATP release (Fig.1B).

To assess whether PA-induced ATP release was related to the activation of the Panx1 channel in renal tubular cells, YoPro-1 fluorescence was monitored in the presence of PA stimulation. The result showed that PA increased YoPro-1 uptake in HK-2 cells compared with control. Interestingly, MT significantly inhibited PA-induced YoPro-1 uptake in HK-2 cells (Fig.2A). Since the Panx1 channel is opened by caspase-3/7 cleavage, we detected the activity of caspase-3/7. Our results showed caspase-3/7 was activated after PA treatment for 24 h in HK-2 cells; MT inhibited the activation (Fig.2B).

eATP aggravated PA-induced monocyte infiltration and inflammatory cytokine release from macrophages and renal tubular cells

To assess whether eATP and PA were capable of inducing migration of monocytes, supernatants from HK-2 cells treated with eATP, PA or eATP plus PA were tested for monocyte migration using a Transwell migration assay. Data show that the supernatants from HK-2 cells treated with PA and to a greater degree with eATP, or eATP plus PA, stimulated THP-1 monocyte migration (upper lane). Compared with the supernatants, the mediums containing eATP, PA or eATP+PA without treating with HK-2 cells had no effects on THP-1 monocyte migration (lower lane) (Fig.3A), suggesting that eATP or PA caused monocyte migration by stimulating chemokine secretion from HK-2 cells. To test this interpretation, we detected the expression of monocyte chemoattractant protein-1 (MCP-1) in HK-2 cells after 24 h treatment with eATP, PA or eATP plus PA. Results showed that both eATP and PA upregulated the mRNA and protein expression of MCP-1 in HK-2 cells; the expression of MCP-1 was much higher in eATP and eATP plus PA-treated HK-2 cells, which was consistent with the chemotaxis induced by the supernatants (Fig.3B and C). Since monocyte

migration could be inhibited by the high concentration of PA and eATP (37), we considered the chemotactic effect of MCP-1 was stronger than the suppression of PA and eATP.

Several studies have demonstrated that PA stimulates IL-1β secretion in THP-1 macrophages (9, 14); however, whether eATP can magnify the PA-induced inflammatory response is still unknown. Hence, supernatants from differentiated THP-1 macrophages treated with eATP, PA or eATP+PA were tested for IL-1β secretion. Notably, compared with eATP or PA only, eATP+PA markedly increased the supernatant IL-1β content as shown by Western blot analysis, suggesting amplification by eATP of the PA-induced inflammatory response in macrophages (Fig.4A).

To assess whether ATP release by PA-triggered HK-2 cells can in turn stimulate the tubular cells to secrete inflammatory cytokines, supernatants from HK-2 cells treated with eATP, PA, or eATP+PA were collected to test IL-1β protein levels. Similar to the macrophages, the supernatant IL-1β level was higher in HK-2 cells treated with eATP+PA than that in the eATP- or PA-treated HK-2 cells, suggesting eATP aggravated PA-induced inflammation in renal tubular cells (Fig.4B).

eATP stimulated IL-1β secretion from THP-1 macrophages and HK-2 cells through the P2X7R-mTOR-FOXO1-TXNIP/NLRP3 inflammasome pathway

Culture supernatants and cell extracts from THP-1 macrophages and HK-2 cells after eATP exposure were collected for testing the mRNA and protein levels of IL-1β and caspase-1. Our results show that eATP increased the mRNA and protein levels of pro-IL-1β significantly, both in THP-1 macrophages (Fig.5A and B) and HK-2 cells (Fig.5C and D), suggesting that eATP can induce the first signal to enhance the transcription and translation of pro-IL-1β. The increased protein levels of mature IL-1β and mature caspase-1 from the supernatants of THP-1 macrophages (Fig.5B and F) and HK-2 cells (Fig.5D and H) suggested that eATP could also act as the

second signal simultaneously for activation of the NLRP3 inflammasome. Though the mRNA level of caspase-1 was elevated, the protein level of pro-caspase-1 did not change significantly in both cell types (Fig.5E, F, G and H), suggesting there may be a balance between the production and the autocatalytic cleavage of pro-caspase-1 that maintained the intracellular protein content of pro-caspase-1. To extend the above findings, A438079 and tunicamycin were used in our experiments to inhibit P2X7R. Interestingly, our data showed that eATP and A438079 had no effect on the expression of P2X7R, while Tm downregulated the protein level of P2X7R in THP-1 macrophages (Fig.6A) and HK-2 cells (Fig.6B). This is consistent with the findings of Lenertz et al. (2010) (23), which suggest that less full-length P2X7R is produced in the presence of Tm, since Tm can inhibit the N-linked glycosylation of P2X7R. However, both A438079 and Tm reduced the mature caspase-1 and mature IL-1β in the supernatant from eATP-treated THP-1 macrophages (Fig.6C) and HK-2 cells (Fig.6D).

Next, we assayed the expression of TXNIP in eATP-treated THP-1 macrophages and HK-2 cells to investigate the activation of the NLRP3 inflammasome. eATP significantly increased the mRNA and the protein levels of TXNIP both in THP-1 macrophages (Fig.7A and B) and HK-2 cells (Fig. 7C and D), suggesting enhanced NLRP3 inflammasome activation resulted from increased combination with TXNIP. However, both A438079 and Tm reduced the mRNA and the protein levels of TXNIP in THP-1 macrophages (Fig.7A and B) and HK-2 cells (Fig. 7C and D).

To gain insight into the mechanisms for the upregulation of TXNIP induced by eATP, we examined the protein level of FOXO1. Results showed eATP markedly increased the protein level of FOXO1 both in THP-1 macrophages (Fig.7E) and HK-2 cells (Fig. 7F), suggesting more FOXO1 bound at the TXNIP promoter, thus promoting the transcription of TXNIP. Furthermore, we found both A438079 and Tm reduced the protein levels of FOXO1 in THP-1 macrophages (Fig.7E) and HK-2 cells (Fig. 7F). Next, we examined the expression of p-mTOR in eATP-treated THP-1 macrophages and HK-2 cells. As shown in the illustration, eATP downregulated the protein level of

p-mTOR significantly; however, both A438079 and Tm upregulated the expression of p-mTOR in THP-1 macrophages (Fig.7G) and HK-2 cells (Fig.7H).

Discussion

It is known and accepted that obesity is associated with, and is a risk factor for, chronic kidney disease (10). Since high circulating NEFA is hallmark of obesity and can mediate many adverse metabolic effects, including insulin resistance, oxidative stress and inflammatory responses (15), we considered whether elevated NEFA levels might be toxic to the kidney and a contributory cause to CKD. In the present study in proximal tubular cells *in vitro*, we found that NEFA overload stimulates ATP release via a mtROS-dependent pathway. The majority of intracellular ROS is produced from mitochondrial respiration and results from the disturbance of the mitochondrial electron transport chain by NEFA (17, 30). The disturbance to the mitochondrial membrane leads to the leakage of electrons to molecular oxygen to produce ROS, which can trigger mitochondrial apoptotic signaling pathways resulting in cell apoptosis (22, 34). Our results demonstrated that PA-induced caspase-3/7 (apoptosis-related cysteine proteases) activation was suppressed by a mtROS inhibitor, suggesting that caspase-3/7 activation might be stimulated by mtROS in renal tubular cells. Since the activated caspase-3/7 can cut the C-terminal of Panx1, leading to the irreversible opening of the human Panx1 channel, detection of the activation of the Panx1 channel was by the YoPro-1 uptake method. Results showed that uptake of YoPro-1 was not detected in healthy HK-2 cells, indicating that Panx1 was not activated in renal tubular cells under normal physiological conditions. Notably, PA caused both YoPro-1 uptake and pathophysiological ATP release, suggesting that the Panx1 channel could be opened by PA stimulation in HK-2 cells. However, the mtROS inhibitor suppressed both YoPro-1 uptake and pathophysiological ATP release, implying the Panx1 channel was closed due to non-activated caspase-3/7 without mtROS production. Therefore, mtROS is the trigger of ATP release during NEFA-induced caspase-3/7 activation, followed by Panx1 channel opening in renal

tubular cells.

It has been reported that the measurable ATP concentration of supernatants is much lower than the amount of ATP release from the cells, because ATP can be rapidly degraded in the bulk phase by extracellular nucleotide enzymes (11). This is likely to be the reason why measurable ATP in the supernatants of HK-2 cells was found to be much lower than the concentrations used *in vitro*. We examined a dose-dependent response of eATP on IL β production, showing that 0.003mM of eATP triggered the secretion of IL-1β, though less than IL-1β secretion caused by 3mM eATP. Therefore, we selected the 3mM eATP as a condition of intervention in the subsequent *in vitro* studies. Normally, the intracellular ATP acts as both an energy source and important signaling molecule. However, when released from the injured cells, eATP exerts its proinflammatory effect and may cause further damage (5).

Next, we showed that eATP aggravated NEFA-induced monocyte infiltration and inflammatory cytokine release from both macrophages and renal tubular cells. It was reported that NEFA-induced ATP release from liver cells can increase MCP-1-mediated monocyte migration (37). In the present study, we demonstrated that eATP functions as an endogenous 'find-me' signal for the recruitment of monocytes in the tubules. Since there is a higher MCP-1 expression in eATP-treated HK-2 cells than in PA-treated HK-2, more monocytes were recruited by the supernatants from HK-2 cells treated with eATP. Stronger chemotaxis caused by eATP suggested that NEFA-induced ATP release may play a more important role than NEFA itself in monocyte recruitment. Furthermore, our study also showed that eATP aggravated PA-increased IL-1β secretion in THP-1 macrophages and HK-2 cells. These data indicate that NEFA-triggered ATP release from renal tubules might generate more severe inflammatory responses in the kidneys of CKD patients.

Finally, eATP aggravated NEFA-induced inflammatory cytokine secretion in macrophages and renal tubular cells through the P2X7R-mTOR-FOXO1-TXNIP/NLRP3 inflammasome pathway. Both animal experiments and clinical studies have revealed that hyperlipidemia is a pathogenic

366 factor for renal inflammation, and lipid-lowering therapy can effectively limit the
367 inflammatory response in CKD (2, 32, 40). However, the mechanisms underlying
368 NEFA-mediated renal tubular inflammation remain ill-defined. The present study
369 shows that PA stimulates IL-1β secretion both in THP-1 macrophages and HK-2 cells,
370 and this inflammatory cytokine release is enhanced by eATP. This suggested that
371 NEFA-triggered ATP release may in turn increase renal tubular inflammation and that
372 eATP might be a potential mediator linked to hyperlipidemia.

373 Next, we examined the mature caspase-1 level, which is an important factor in
374 NLRP3 inflammasome activation. Results showed that eATP increases both mRNA
375 and mature protein levels of caspase-1, and that this can be inhibited by P2X7R
376 inhibitors, suggesting the NLRP3 inflammasome is activated by eATP in macrophages
377 and renal tubular cells involving the P2X7R pathway. Furthermore, we also
378 demonstrated that eATP-induced TXNIP upregulation played an important role in
379 NLRP3 inflammasome activation, leading to the cleavage and release of IL-1β both in
380 both macrophages and renal tubular cells. As a transcription factor of TXNIP, the
381 FOXO1 protein level was also elevated by eATP. Notably, the downregulation of
382 TXNIP and FOXO1 caused by the P2X7R inhibitor was consistnet with eATP release
383 functioning as an endogenous danger signal for tubular inflammation by increasing
384 TXNIP in macrophages and renal tubular cells. Interestingly, FOXO1 is also an IL-1β
385 transcription factors. Hence, FOXO1 may increase transcription, in addition to
386 cleavage of IL-1β, in the presence of eATP. Nevertheless, activation of NF-κB may
387 account for the increased expression of IL-1β induced by both PA and eATP (27, 31),
388 since NF-κB is an important transcription factor for IL-1β.

389 mTOR is known to play a central role in many critical cellular processes such as
390 proliferation, survival, autophagy, inflammation and metabolism. P2X7R suppresses
391 mTOR by inhibiting phosphoinositide-3-kinase (PI3K)/serine/threonine kinase (AKT)
392 and activating the adenosine 5'-monophosphate-activated protein kinase (AMPK)
393 signaling pathway to effect tumor cell death (4). We detected p-mTOR protein levels
394 since mTOR is an important modulator of FOXO1. eATP downregulated the protein

level of p-mTOR, which could be reversed by A438079 and Tm, indicating that P2X7R activation can suppress the mTOR signaling network. Hence we propose, and a subject for further investigation, that eATP-P2X7R regulates mTOR via PI3K/AKT or AMPK signaling, which may play an important role in renal tubular inflammation. We conclude that eATP triggered NLRP3 inflammasome activation through the P2X7R-mTOR-FOXO1-TXNIP/NLRP3 inflammasome pathway, resulting in the release of IL-1β from both macrophages and renal tubular cells.

In summary, NEFA increase mtROS production and inflammatory stress, causing the 'first hit'. The first hit stimulates ATP release from Panx1 channel on renal tubules by activation of caspase-3/7. Then, acting as the 'second hit', eATP aggravates the tubular inflammatory response by increasing monocyte infiltration and stimulating inflammatory cytokine release from both macrophage and renal tubular cells via the P2X7R-mTOR-FOXO1-TXNIP/NLRP3 inflammasome pathway (Fig.8). This may cause a severe renal inflammatory response and renal dysfunction. Thus, inhibition of ATP release and/or P2X7-mediated actions may be a potential means of alleviating renal inflammation to improve renal function.

Acknowledgments: Address all correspondence and requests for reprints to Xiong Zhong Ruan, Director, John Moorhead Research Laboratory, Centre for Nephrology, University College London (UCL) Medical School, Royal Free Campus, London, NW3 2PF, UK. E-mail: x.ruan@ucl.ac.uk. Robert Unwin is Emeritus Professor of Nephrology at UCL and is currently working in Early Clinical Development, Early CVRM (Cardiovascular, Renal and Metabolism), R&D BioPharmaceuticals, AstraZeneca, Cambridge, UK and Gothenburg, Sweden.

Grants: This work was supported by grants from National Natural Science Youth Foundation of China (81700632 to HS), National Key R&D Program of China (2018 YFC1312700), the Natural Science Youth Foundation of Jiangsu Province

(BK20170366 to HS), and the China Scholarship Council (CSC) (201406090317), Moorhead Trust.

Disclosure: The authors have nothing to disclose, other than RU's employment by AstraZeneca.

Reference

1. **Abais JM, Xia M, Li G, Chen Y, Conley SM, Gehr TW, Boini KM, and Li PL.** Nod-like receptor protein 3 (NLRP3) inflammasome activation and podocyte injury via thioredoxin-interacting protein (TXNIP) during hyperhomocysteinemia. *The Journal of biological chemistry* 289: 27159-27168, 2014.
2. **Almquist T, Jacobson SH, Mobarrez F, Nasman P, and Hjemdahl P.** Lipid-lowering treatment and inflammatory mediators in diabetes and chronic kidney disease. *European journal of clinical investigation* 44: 276-284, 2014.
3. **Baines RJ, Chana RS, Hall M, Febbraio M, Kennedy D, and Brunskill NJ.** CD36 mediates proximal tubular binding and uptake of albumin and is upregulated in proteinuric nephropathies. *American journal of physiology Renal physiology* 303: F1006-1014, 2012.
4. **Bian S, Sun X, Bai A, Zhang C, Li L, Enjyoji K, Junger WG, Robson SC, and Wu Y.** P2X7 integrates PI3K/AKT and AMPK-PRAS40-mTOR signaling pathways to mediate tumor cell death. *PloS one* 8: e60184, 2013.
5. **Chekeni FB, Elliott MR, Sandilos JK, Walk SF, Kinchen JM, Lazarowski ER, Armstrong AJ, Penuela S, Laird DW, Salvesen GS, Isakson BE, Bayliss DA, and Ravichandran KS.** Pannexin 1 channels mediate 'find-me' signal release and membrane permeability during apoptosis. *Nature* 467: 863-867, 2010.
6. **Chen B, Xu X, Luo J, Wang H, and Zhou S.** Rapamycin Enhances the Anti-Cancer Effect of Dasatinib by Suppressing Src/PI3K/mTOR Pathway in NSCLC Cells. *PloS one* 10: e0129663, 2015.
7. **Christensen EI and Birn H.** Megalin and cubilin: synergistic endocytic receptors in renal proximal tubule. *American journal of physiology Renal physiology* 280: F562-573, 2001.
8. **Dahl G.** ATP release through pannexon channels. *Philosophical transactions of the Royal Society of London Series B, Biological sciences* 370, 2015.
9. **Dasu MR and Jialal I.** Free fatty acids in the presence of high glucose amplify monocyte inflammation via Toll-like receptors. *American journal of physiology Endocrinology and metabolism* 300: E145-154, 2011.
10. **Decleves AE and Sharma K.** Obesity and kidney disease: differential effects of obesity on adipose tissue and kidney inflammation and fibrosis. *Current opinion in nephrology and hypertension* 24: 28-36, 2015.
11. **Dou L, Chen YF, Cowan PJ, and Chen XP.** Extracellular ATP signaling and clinical relevance. *Clin Immunol* 188: 67-73, 2018.
12. **Dourado M, Wong E, and Hackos DH.** Pannexin-1 is blocked by its C-terminus through a delocalized non-specific interaction surface. *PloS one* 9: e99596, 2014.
13. **Ferrari D, Pizzirani C, Adinolfi E, Lemoli RM, Curti A, Idzko M, Panther E, and Di Virgilio F.** The P2X7 receptor: a key player in IL-1 processing and release. *J Immunol* 176: 3877-3883, 2006.
14. **Fu L, Zhou F, Wang X, and Lu F.** [Effect of free fatty acid on NALP3 inflammasome signaling pathway in THP-1 macrophages]. *Zhong nan da xue xue bao Yi xue ban = Journal of Central South University Medical sciences* 39: 811-817,

2014.
15. **Gai Z, Wang T, Visentin M, Kullak-Ublick GA, Fu X, and Wang Z.** Lipid Accumulation and Chronic Kidney Disease. *Nutrients* 11, 2019.
16. **Gorriz JL and Martinez-Castelao A.** Proteinuria: detection and role in native renal disease progression. *Transplant Rev (Orlando)* 26: 3-13, 2012.
17. **Graciano MF, Valle MM, Kowluru A, Curi R, and Carpinelli AR.** Regulation of insulin secretion and reactive oxygen species production by free fatty acids in pancreatic islets. *Islets* 3: 213-223, 2011.
18. **Hsu CK, Lin CC, Hsiao LD, and Yang CM.** Mevastatin ameliorates sphingosine 1-phosphate-induced COX-2/PGE2-dependent cell migration via FoxO1 and CREB phosphorylation and translocation. *British journal of pharmacology* 172: 5360-5376, 2015.
19. **Impellizzeri D, Esposito E, Attley J, and Cuzzocrea S.** Targeting inflammation: new therapeutic approaches in chronic kidney disease (CKD). *Pharmacological research : the official journal of the Italian Pharmacological Society* 81: 91-102, 2014.
20. **Kibbe C, Chen J, Xu G, Jing G, and Shalev A.** FOXO1 competes with carbohydrate response element-binding protein (ChREBP) and inhibits thioredoxin-interacting protein (TXNIP) transcription in pancreatic beta cells. *The Journal of biological chemistry* 288: 23194-23202, 2013.
21. **Koyama T, Kume S, Koya D, Araki S, Isshiki K, Chin-Kanasaki M, Sugimoto T, Haneda M, Sugaya T, Kashiwagi A, Maegawa H, and Uzu T.** SIRT3 attenuates palmitate-induced ROS production and inflammation in proximal tubular cells. *Free radical biology & medicine* 51: 1258-1267, 2011.
22. **Lawal AO, Marnewick JL, and Ellis EM.** Heme oxygenase-1 attenuates cadmium-induced mitochondrial-caspase 3- dependent apoptosis in human hepatoma cell line. *BMC pharmacology & toxicology* 16: 41, 2015.
23. **Lenertz LY, Wang Z, Guadarrama A, Hill LM, Gavala ML, and Bertics PJ.** Mutation of putative N-linked glycosylation sites on the human nucleotide receptor P2X7 reveals a key residue important for receptor function. *Biochemistry* 49: 4611-4619, 2010.
24. **Lerner AG, Upton JP, Praveen PV, Ghosh R, Nakagawa Y, Igbaria A, Shen S, Nguyen V, Backes BJ, Heiman M, Heintz N, Greengard P, Hui S, Tang Q, Trusina A, Oakes SA, and Papa FR.** IRE1alpha induces thioredoxin-interacting protein to activate the NLRP3 inflammasome and promote programmed cell death under irremediable ER stress. *Cell metabolism* 16: 250-264, 2012.
25. **Li X, Kover KL, Heruth DP, Watkins DJ, Moore WV, Jackson K, Zang M, Clements MA, and Yan Y.** New Insight Into Metformin Action: Regulation of ChREBP and FOXO1 Activities in Endothelial Cells. *Mol Endocrinol* 29: 1184-1194, 2015.
26. **Maiese K, Chong ZZ, Hou J, and Shang YC.** The "O" class: crafting clinical care with FoxO transcription factors. *Advances in experimental medicine and biology* 665: 242-260, 2009.
27. **Mezzasoma L, Antognelli C, and Talesa VN.** Atrial natriuretic peptide

down-regulates LPS/ATP-mediated IL-1beta release by inhibiting NF-kB, NLRP3 inflammasome and caspase-1 activation in THP-1 cells. *Immunologic research* 64: 303-312, 2016.

28. **Puthanveetil P, Wan A, and Rodrigues B.** FoxO1 is crucial for sustaining cardiomyocyte metabolism and cell survival. *Cardiovascular research* 97: 393-403, 2013.

29. **Rodriguez-Iturbe B and Garcia Garcia G.** The role of tubulointerstitial inflammation in the progression of chronic renal failure. *Nephron Clinical practice* 116: c81-88, 2010.

30. **Schonfeld P and Wojtczak L.** Fatty acids as modulators of the cellular production of reactive oxygen species. *Free radical biology & medicine* 45: 231-241, 2008.

31. **Shi X, Li D, Deng Q, Li Y, Sun G, Yuan X, Song Y, Wang Z, Li X, and Liu G.** NEFAs activate the oxidative stress-mediated NF-kappaB signaling pathway to induce inflammatory response in calf hepatocytes. *The Journal of steroid biochemistry and molecular biology* 145: 103-112, 2015.

32. **Sleeman P, Patel NN, Lin H, Walkden GJ, Ray P, Welsh GI, Satchell SC, and Murphy GJ.** High fat feeding promotes obesity and renal inflammation and protects against post cardiopulmonary bypass acute kidney injury in swine. *Crit Care* 17: R262, 2013.

33. **Soumura M, Kume S, Isshiki K, Takeda N, Araki S, Tanaka Y, Sugimoto T, Chin-Kanasaki M, Nishio Y, Haneda M, Koya D, Kashiwagi A, Maegawa H, and Uzu T.** Oleate and eicosapentaenoic acid attenuate palmitate-induced inflammation and apoptosis in renal proximal tubular cell. *Biochemical and biophysical research communications* 402: 265-271, 2010.

34. **Tanaka Y, Kume S, Araki H, Nakazawa J, Chin-Kanasaki M, Araki S, Nakagawa F, Koya D, Haneda M, Maegawa H, and Uzu T.** 1-Methylnicotinamide ameliorates lipotoxicity-induced oxidative stress and cell death in kidney proximal tubular cells. *Free radical biology & medicine* 89: 831-841, 2015.

35. **Thomas ME and Schreiner GF.** Contribution of proteinuria to progressive renal injury: consequences of tubular uptake of fatty acid bearing albumin. *American journal of nephrology* 13: 385-398, 1993.

36. **van der Vusse GJ.** Albumin as fatty acid transporter. *Drug metabolism and pharmacokinetics* 24: 300-307, 2009.

37. **Xiao F, Waldrop SL, Bronk SF, Gores GJ, Davis LS, and Kilic G.** Lipoapoptosis induced by saturated free fatty acids stimulates monocyte migration: a novel role for Pannexin1 in liver cells. *Purinergic signalling* 11: 347-359, 2015.

38. **Xiao F, Waldrop SL, Khimji AK, and Kilic G.** Pannexin1 contributes to pathophysiological ATP release in lipoapoptosis induced by saturated free fatty acids in liver cells. *American journal of physiology Cell physiology* 303: C1034-1044, 2012.

39. **Yamaguchi F, Hirata Y, Akram H, Kamitori K, Dong Y, Sui L, and Tokuda M.** FOXO/TXNIP pathway is involved in the suppression of hepatocellular carcinoma growth by glutamate antagonist MK-801. *BMC cancer* 13: 468, 2013.

40. **Yao L, Li L, Li X, Li H, Zhang Y, Zhang R, Wang J, and Mao X.** The anti-inflammatory and antifibrotic effects of Coreopsis tinctoria Nutt on high-glucose-fat diet and streptozotocin-induced diabetic renal damage in rats. *BMC complementary and alternative medicine* 15: 314, 2015.
41. **Zhou R, Tardivel A, Thorens B, Choi I, and Tschopp J.** Thioredoxin-interacting protein links oxidative stress to inflammasome activation. *Nature immunology* 11: 136-140, 2010.

Fig 1 (A) PA induced mtROS production in HK-2 cells. (B) PA induced ATP release from HK-2 cells. HK-2 cells were treated with experimental medium (Ctr) and medium in the presence of 3.2mM PA (PA), PA plus 10μM MT (PA+MT), or MT (MT) alone. After 24 h incubation, mtROS production was determined using dihydroethidium, and cells were observed under a fluorescence microscope. Original magnification, 400×. The mtROS production was quantified by Carl Zeiss Aim software. Values are mean ± SEM from 3 separate fields, expressed as a percentage of Ctr. The supernatant ATP was detected by ATP Assay Kit. The histogram represents mean ± SEM of the supernatant ATP concentration from 5 experiments, expressed as a percentage of Ctr. $^{*}P< 0.05$, compared with Ctr; $^{\#}P < 0.05$, compared with PA.

Fig 2 (A) PA induced YoPro-1 uptake in HK-2 cells. (B) PA induced caspase-3/7 activation in HK-2 cells. HK-2 cells were treated with experimental medium (Ctr) and medium in the presence of 3.2mM PA (PA), PA plus 10μM MT (PA+MT), or MT (MT) alone. After 24 h incubation, Panx1 activation was measured by YoPro-1 fluorescence, and caspase-3/7 activation was tested by CellEvent™ Caspase-3/7 Green ReadyProbes® Reagent. After that, cells were observed under a fluorescence microscope. Original magnification, 400×.The YoPro-1 uptake and caspase-3/7 activation were quantified by Carl Zeiss Aim software. Values are mean ± SEM from 3 separate fields, expressed as a percentage of Ctr. $^{*}P< 0.05$, compared with Ctr; $^{\#}P < 0.05$, compared with PA.

Fig 3 (A) eATP aggravated PA-induced THP-1 monocyte migration. (B) eATP aggravated PA-induced mRNA level of MCP-1 in HK-2 cells. (C) eATP aggravated PA-induced protein level of MCP-1 in HK-2 cells. HK-2 cells were treated with experimental medium (Ctr) and medium in the presence of 3mM eATP (eATP), 3.2mM PA (PA) or eATP plus PA (eATP+PA). After 24 h incubation, culture

supernatants (sCtr, seATP, sPA and seATP+PA) were harvested and used for the chemotaxis assay. The mediums containing eATP, PA, or eATP+PA (not incubated with HK-2 cells) were used as references. Original magnification, 200×. The histogram represents mean ± SEM of the THP-1 monocyte counts from 5 experiments. Total RNA was isolated and the mRNA level of MCP-1 was detected. β-actin served as a reference gene. The supernatant MCP-1 protein content was detected by ELISA kit. The histogram represent the mean ± SEM from 5 experiments, expressed as a percentage of Ctr. *P< 0.05, compared with Ctr; $^{\#}P$< 0.05, compared with PA.

Fig 4 (A) eATP aggravated PA-induced IL-1β secretion in THP-1 macrophages. THP-1 macrophages were treated with experimental medium (Ctr) and medium in the presence of 3mM eATP (eATP), 3.2mM PA (PA) or eATP plus PA (eATP+PA). After 24 h incubation, culture supernatants were harvested and used for testing mature IL-1β protein level by using western blot analysis. (B) eATP aggravated PA-induced IL-1β secretion in HK-2 cells. HK-2 cells were treated with experimental medium (Ctr) and medium in the presence of 3mM eATP (eATP), 3.2mM PA (PA) or eATP plus PA (eATP+PA). After 24 h incubation, culture supernatants were harvested and used for testing mature IL-1β protein level by using western blot analysis. The histogram represents mean ± SEM of the densitometric scans for proteins from 5 experiments, normalized by comparison with β-actin and expressed as a percentage of Ctr. *P< 0.05, compared with Ctr; $^{\blacktriangle}P$< 0.05, compared with eATP; $^{\#}P$< 0.05, compared with PA.

Fig 5 (A) eATP increased the mRNA level of IL-1β in THP-1 macrophages. (B) eATP increased the protein levels of both pro-IL-1β and mature IL-1β in THP-1 macrophages. (C) eATP increased the mRNA level of IL-1β in HK-2 cells. (D) eATP increased the protein levels of both pro-IL-1β and mature IL-1β in HK-2 cells. (E) eATP increased the mRNA level of caspase-1 in THP-1 macrophages. (F) eATP

643 increased the protein level of mature caspase-1 in THP-1 macrophages. (G) eATP
644 increased the mRNA level of caspase-1 in HK-2 cells. (H) eATP increased the protein
645 level of mature caspase-1 in HK-2 cells. THP-1 macrophages or HK-2 cells were
646 treated with experimental medium (Ctr) and 3mM eATP. After 24 h incubation, total
647 RNA was isolated and the mRNA levels were detected. β-actin served as a reference
648 gene. Culture supernatants and cell extracts were collected and used for testing
649 protein levels by western blot analysis. The protein levels were normalized by
650 comparison with β-actin. The histogram represents the mean ± SEM from 5
651 experiments, expressed as a percentage of Ctr. *P< 0.05, compared with Ctr; ns = not
652 significant, compared with Ctr.

653

654 Fig 6 (A) Tm reduced the protein level of P2X7R in THP-1 macrophages. (B) Tm
655 reduced the protein level of P2X7R in HK-2 cells. (C) A438079 and Tm reduced the
656 protein levels of mature caspase-1 and IL-1β in THP-1 macrophages. (D) A438079
657 and Tm reduced the protein levels of mature caspase-1 and IL-1β in HK-2 cell. THP-1
658 macrophages or HK-2 cells were treated with experimental medium (Ctr) and medium
659 in the presence of 3mM eATP (eATP), eATP plus 50μM A438079 (eATP+A438079)
660 or eATP plus 1μg/ml Tm (eATP+Tm). After 24 h incubation, total RNA was isolated
661 and the mRNA levels were detected. β-actin served as a reference gene. Culture
662 supernatants and cell extracts were collected and used for testing protein levels by
663 western blot analysis. The protein levels were normalized by comparison with β-actin.
664 The histogram represent the mean ± SEM from 5 experiments, expressed as a
665 percentage of Ctr. *P< 0.05, compared with Ctr; ▲P< 0.05, compared with eATP.

666

667 Fig 7 (A) eATP increased the mRNA level of TXNIP in THP-1 macrophages. (B)
668 eATP increased the protein level of TXNIP in THP-1 macrophages. (C) eATP
669 increased the mRNA level of TXNIP in HK-2 cells. (D) eATP increased the protein
670 level of TXNIP in HK-2 cells. (E) eATP increased the protein level of FOXO1 in

THP-1 macrophages. (F) eATP increased the protein level of FOXO1 in HK-2 cells. (G) eATP increased the protein level of p-mTOR in THP-1 macrophages. (H) eATP increased the protein level of p-mTOR in HK-2 cells. THP-1 macrophages or HK-2 cells were treated with experimental medium (Ctr) and medium in the presence of 3mM eATP (eATP), eATP plus 50μM A438079 (eATP+A438079) or eATP plus 1μg/ml Tm (eATP+Tm). After 24 h incubation, total RNA was isolated and the mRNA levels were detected. β-actin served as a reference gene. Culture supernatants and cell extracts were collected and used for testing protein levels by western blot analysis. The protein levels were normalized by comparison with β-actin. The histogram represent the mean ± SEM from 5 experiments, expressed as a percentage of Ctr. *$P<$ 0.05, compared with Ctr; ▲$P<$ 0.05, compared with eATP.

Fig 8 Amplification and enhancement of inflammatory responses in renal tubules. ① NEFA induces mtROS-dependent caspase-3/7 activation in renal tubular cells, and then, the activated caspase-3/7 opens the Panx1 channel, leading to pathophysiological ATP release. ②Both eATP and NEFA increase the secretion of MCP-1 from renal tubular cells, which induce monocyte infiltration. ③NEFA stimulates IL-1β release from both macrophages and renal tubular cells. ④eATP stimulates IL-1β release from both macrophages renal tubular cells via the P2X7R-mTOR-FOXO1-TXNIP/NLRP3 inflammasome pathway. eATP-P2X7R negatively regulates mTOR, which increases the expression of FOXO1. The upregulated FOXO1 enters the nucleus, binds to the promoter of TXNIP, resulting in the enhanced transcription and translation of TXNIP. Then, the increased TXNIP binds to the NLRP3 inflammasome, causes the activation of the NLRP3 inflammasome, followed by the autocatalytic cleavage of pro-caspase-1 to caspase-1. Then, the caspase-1 cleaves the inactive precursor of IL-1β into its biologically active form.

699

700 **Table.1 The primers for real-time RT-PCR.**

701 MCP-1, monocyte chemoattractant protein-1; IL-1β, interleukin-1β; TXNIP,
702 thioredoxin-interacting protein.

703

Gene	Primers
MCP-1	5'- CCATTGTGGCCAAGGAGATC -3' sense
	5'- TGTCCAGGTGGTCCATGGA -3' antisense
Caspase-1	5'- GCTTTCTGCTCTTCCACACC -3' sense
	5'- CATCTGGCTGCTCAAATGAA -3' antisense
IL-1β	5'- ATCCCATCCCAACACACAC -3' sense
	5'- TCTTTCAACACGCAGGACAG -3' antisense
TXNIP	5'- ACTCGTGTCAAAGCCGTTAGG -3' sense
	5'- TCCCTGCATCCAAAGCACTT -3' antisense
β-actin	5'- AGCGAGCATCCCCCAAAGTT -3' sense
	5'- GGGCACGAAGGCTCATCATT -3' antisense

704

705

Fig 1

A

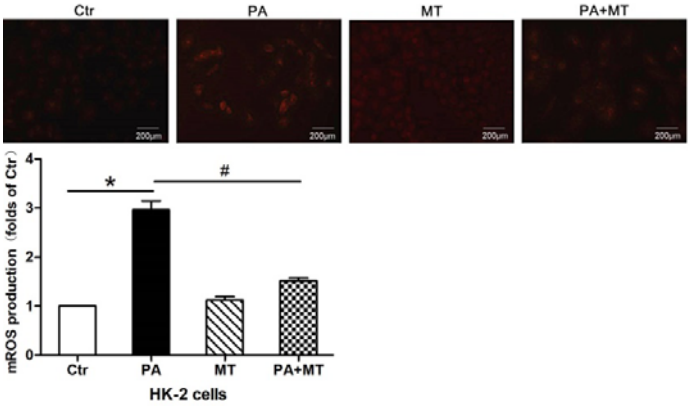
Ctr
PA
MT
PA+MT
200μm
mROS production（folds of Ctr）
0
1
2
3
4
*
#
Ctr
PA
MT
PA+MT
HK-2 cells

B

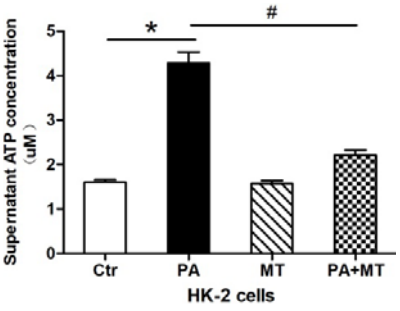
Supernatant ATP concentration
（uM）
0
1
2
3
4
5
*
#
Ctr
PA
MT
PA+MT
HK-2 cells

Fig 2

A

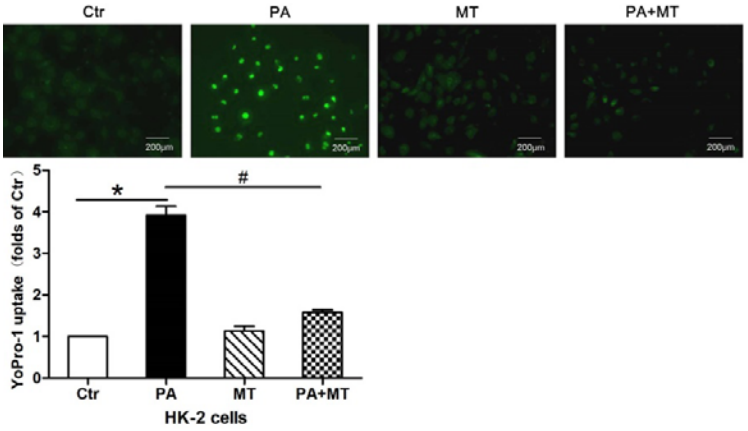
Ctr
PA
MT
PA+MT
200μm
YoPro-1 uptake（folds of Ctr）
0
1
2
3
4
5
*
#
Ctr
PA
MT
PA+MT
HK-2 cells

B

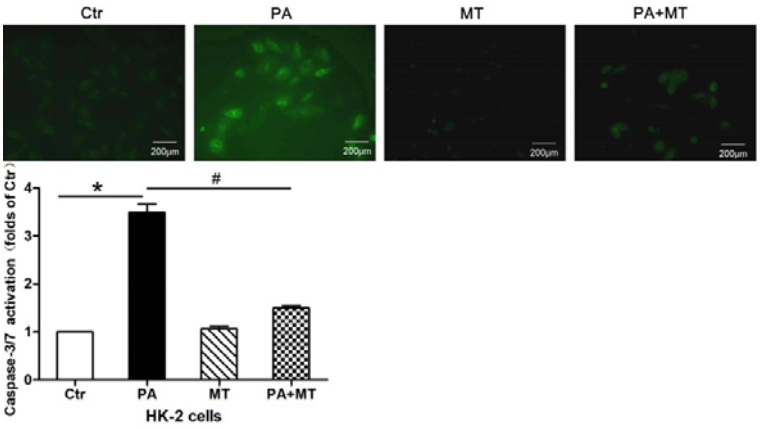
Ctr
PA
MT
PA+MT
200μm
Caspase-3/7 activation（folds of Ctr）
0
1
2
3
4
*
#
Ctr
PA
MT
PA+MT
HK-2 cells

Fig 3

A

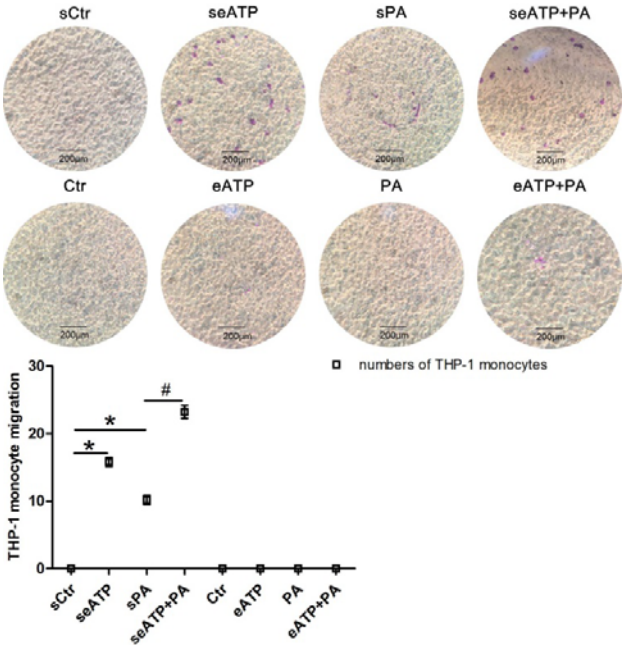
sCtr
seATP
sPA
seATP+PA
Ctr
eATP
PA
eATP+PA
numbers of THP-1 monocytes
THP-1 monocyte migration
30
20
10
0
*
*
#
sCtr
seATP
sPA
seATP+PA
Ctr
eATP
PA
eATP+PA

B

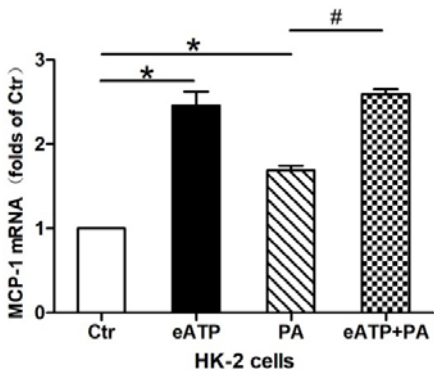
MCP-1 mRNA（folds of Ctr）
3
2
1
0
*
*
#
Ctr
eATP
PA
eATP+PA
HK-2 cells

C

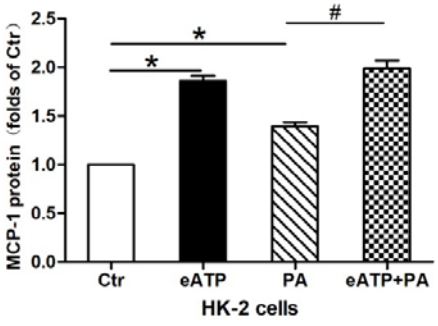
MCP-1 protein（folds of Ctr）
2.5
2.0
1.5
1.0
0.5
0.0
*
*
#
Ctr
eATP
PA
eATP+PA
HK-2 cells

Fig 4

A

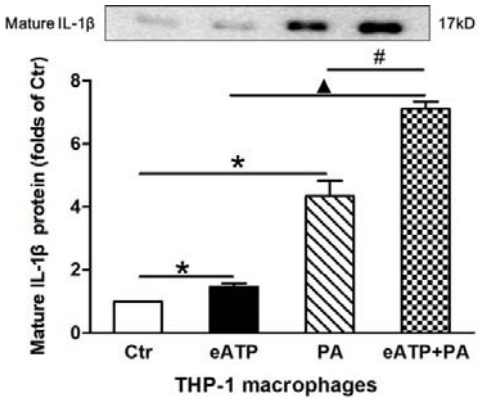
Mature IL-1β
17kD
Mature IL-1β protein (folds of Ctr)
0
2
4
6
8
*
*
#
Ctr
eATP
PA
eATP+PA
THP-1 macrophages

B

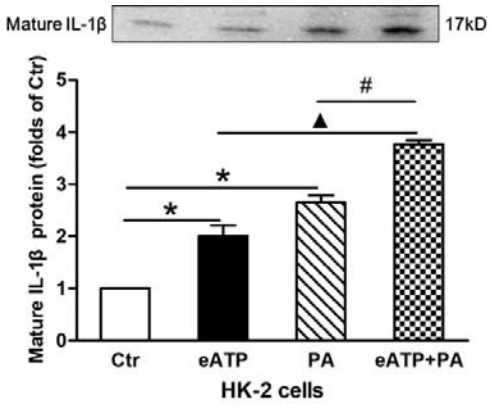
Mature IL-1β
17kD
Mature IL-1β protein (folds of Ctr)
0
1
2
3
4
5
*
*
#
Ctr
eATP
PA
eATP+PA
HK-2 cells

Fig 5

A

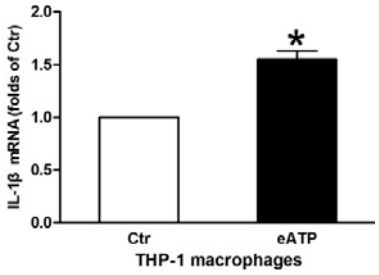
IL-1β mRNA (folds of Ctr)
2.0
1.5
1.0
0.5
0.0
*
Ctr
eATP
THP-1 macrophages

B

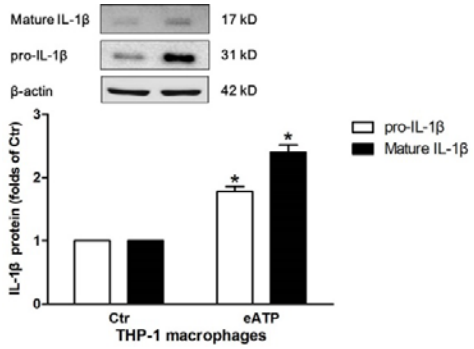
Mature IL-1β
17 kD
pro-IL-1β
31 kD
β-actin
42 kD
IL-1β protein (folds of Ctr)
3
2
1
0
*
*
pro-IL-1β
Mature IL-1β
Ctr
eATP
THP-1 macrophages

C

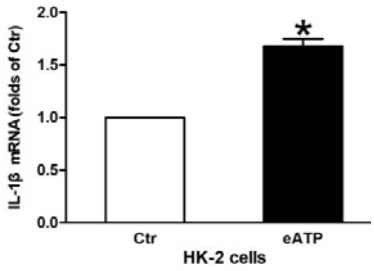
IL-1β mRNA (folds of Ctr)
2.0
1.5
1.0
0.5
0.0
*
Ctr
eATP
HK-2 cells

D

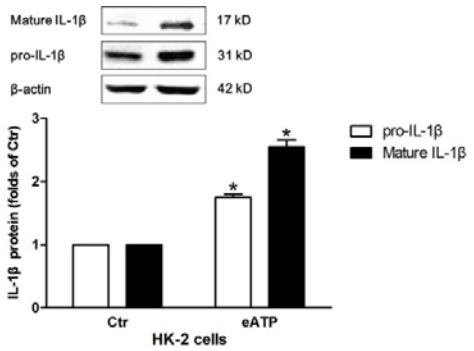
Mature IL-1β
17 kD
pro-IL-1β
31 kD
β-actin
42 kD
IL-1β protein (folds of Ctr)
3
2
1
0
*
*
pro-IL-1β
Mature IL-1β
Ctr
eATP
HK-2 cells

E

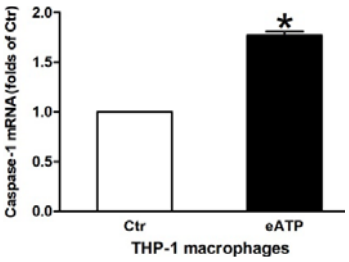
Caspase-1 mRNA (folds of Ctr)
2.0
1.5
1.0
0.5
0.0
*
Ctr
eATP
THP-1 macrophages

F

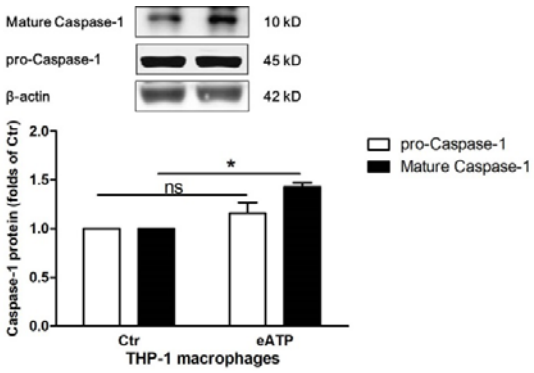
Mature Caspase-1
10 kD
pro-Caspase-1
45 kD
β-actin
42 kD
Caspase-1 protein (folds of Ctr)
2.0
1.5
1.0
0.5
0.0
*
ns
Ctr
eATP
THP-1 macrophages
pro-Caspase-1
Mature Caspase-1

G

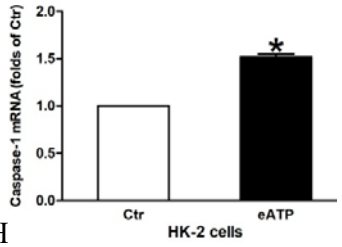
Caspase-1 mRNA (folds of Ctr)
2.0
1.5
1.0
0.5
0.0
*
Ctr
eATP
HK-2 cells

H

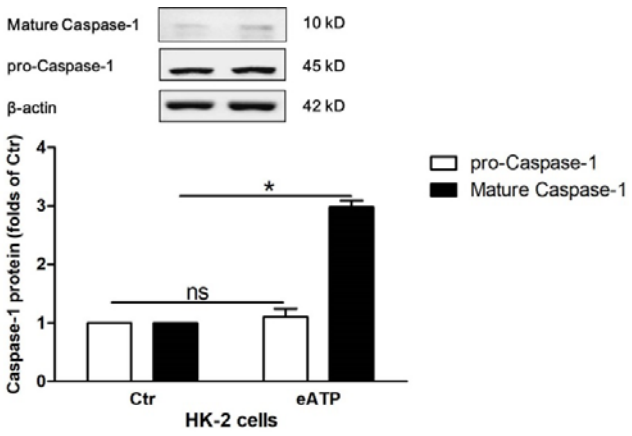
Mature Caspase-1
10 kD
pro-Caspase-1
45 kD
β-actin
42 kD
Caspase-1 protein (folds of Ctr)
4
3
2
1
0
*
ns
Ctr
eATP
HK-2 cells
pro-Caspase-1
Mature Caspase-1

Fig 6

A

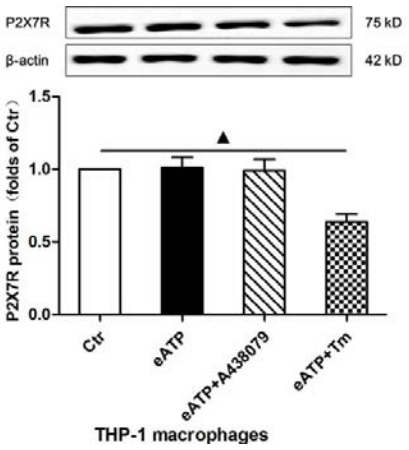
P2X7R
75 kD
β-actin
42 kD
P2X7R protein（folds of Ctr）
1.5
1.0
0.5
0.0
Ctr
eATP
eATP+A438079
eATP+Tm
THP-1 macrophages

B

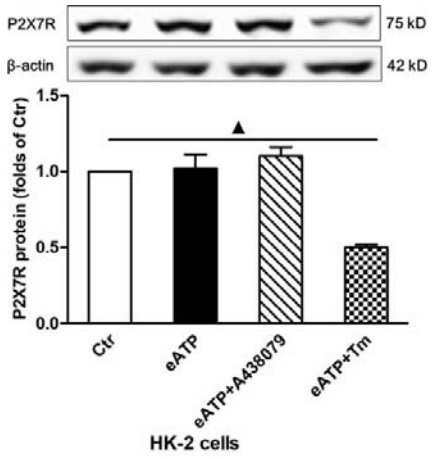
P2X7R
75 kD
β-actin
42 kD
P2X7R protein (folds of Ctr)
1.5
1.0
0.5
0.0
Ctr
eATP
eATP+A438079
eATP+Tm
HK-2 cells

C

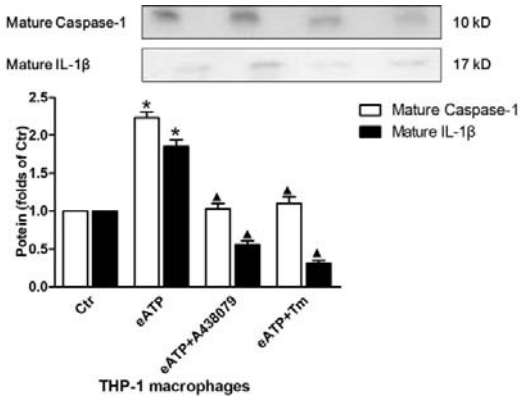
Mature Caspase-1
10 kD
Mature IL-1β
17 kD
Mature Caspase-1
Mature IL-1β
Potein (folds of Ctr)
2.5
2.0
1.5
1.0
0.5
0.0
Ctr
eATP
eATP+A438079
eATP+Tm
THP-1 macrophages

D

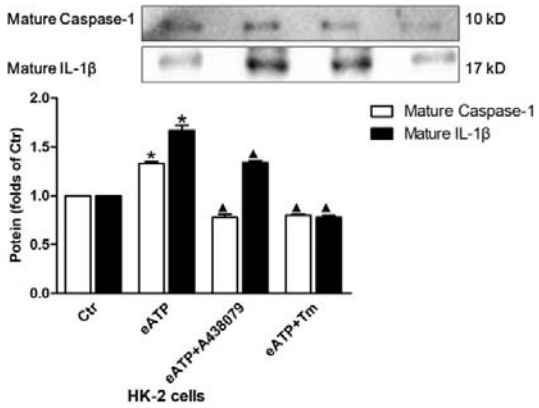
Mature Caspase-1
10 kD
Mature IL-1β
17 kD
Mature Caspase-1
Mature IL-1β
Potein (folds of Ctr)
2.0
1.5
1.0
0.5
0.0
Ctr
eATP
eATP+A438079
eATP+Tm
HK-2 cells

Fig 7

A

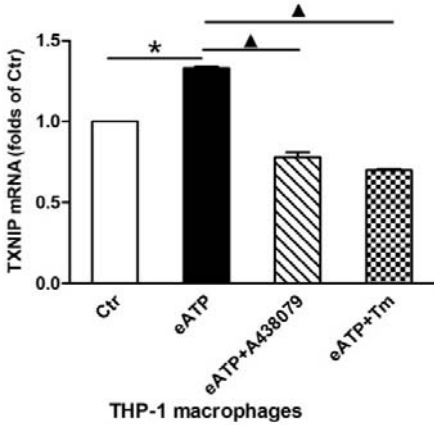
TXNIP mRNA (folds of Ctr)
1.5
1.0
0.5
0.0
*
▲
▲
Ctr
eATP
eATP+A438079
eATP+Tm
THP-1 macrophages

B

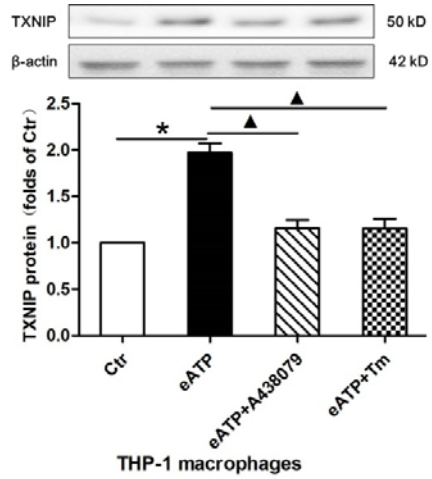
TXNIP
50 kD
β-actin
42 kD
TXNIP protein（folds of Ctr）
2.5
2.0
1.5
1.0
0.5
0.0
*
▲
▲
Ctr
eATP
eATP+A438079
eATP+Tm
THP-1 macrophages

C

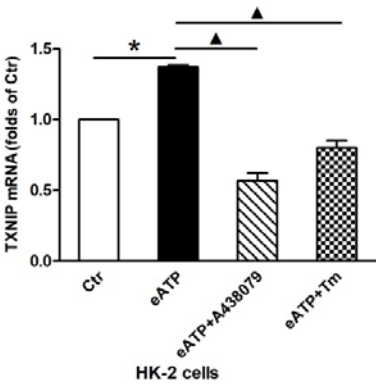
TXNIP mRNA (folds of Ctr)
1.5
1.0
0.5
0.0
*
▲
▲
Ctr
eATP
eATP+A438079
eATP+Tm
HK-2 cells

D

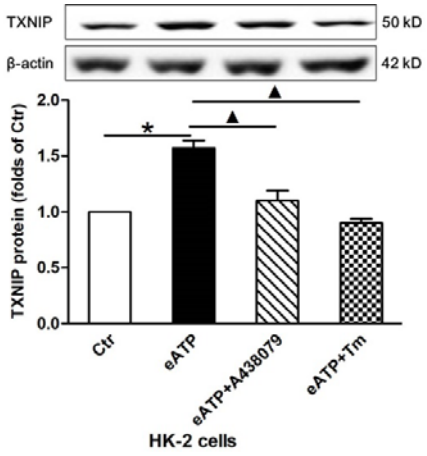
TXNIP
50 kD
β-actin
42 kD
TXNIP protein (folds of Ctr)
2.0
1.5
1.0
0.5
0.0
*
Ctr
eATP
eATP+A438079
eATP+Tm
HK-2 cells

E

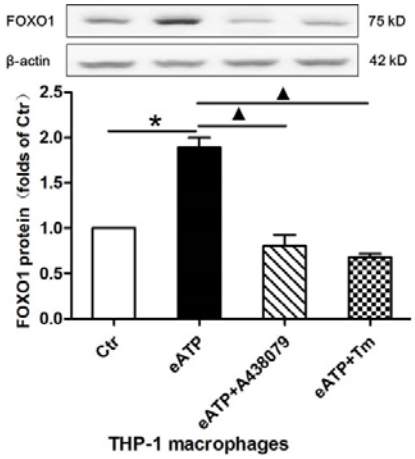
FOXO1
75 kD
β-actin
42 kD
FOXO1 protein（folds of Ctr）
2.5
2.0
1.5
1.0
0.5
0.0
*
Ctr
eATP
eATP+A438079
eATP+Tm
THP-1 macrophages

F

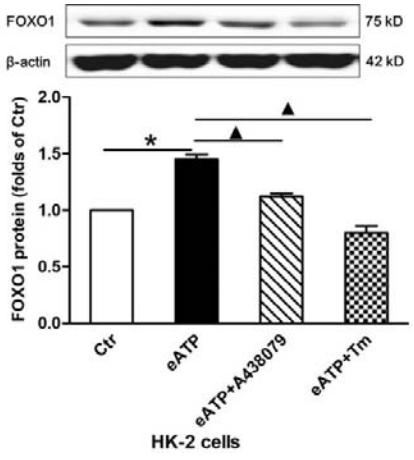
FOXO1
75 kD
β-actin
42 kD
FOXO1 protein (folds of Ctr)
2.0
1.5
1.0
0.5
0.0
*
Ctr
eATP
eATP+A438079
eATP+Tm
HK-2 cells

G

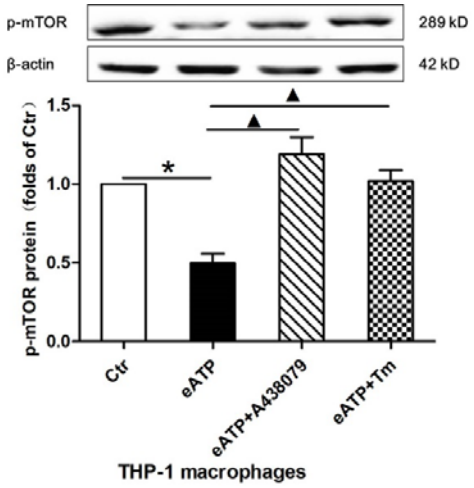
p-mTOR
289 kD
β-actin
42 kD
p-mTOR protein（folds of Ctr）
1.5
1.0
0.5
0.0
*
Ctr
eATP
eATP+A438079
eATP+Tm
THP-1 macrophages

H

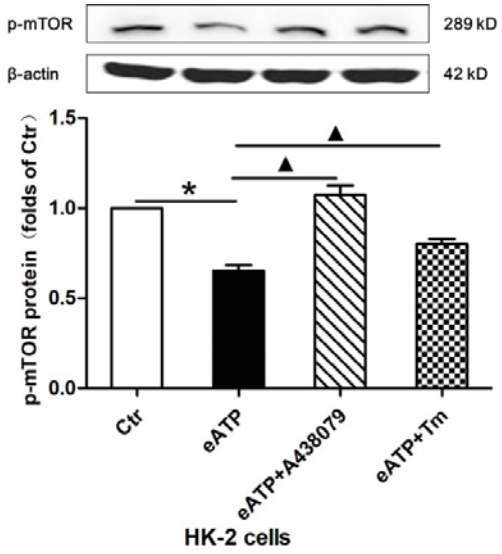
p-mTOR
289 kD
β-actin
42 kD
p-mTOR protein（folds of Ctr）
1.5
1.0
0.5
0.0
*
Ctr
eATP
eATP+A438079
eATP+Tm
HK-2 cells

Fig 8

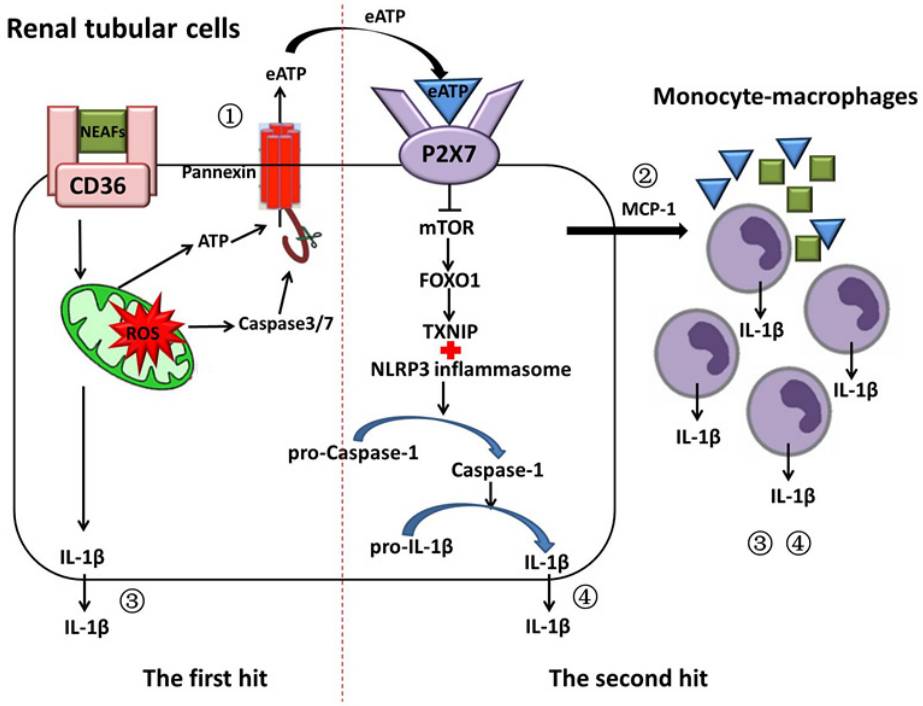
Renal tubular cells
eATP
eATP
eATP
①
NEAFs
CD36
Pannexin
P2X7
Monocyte-macrophages
②
MCP-1
ATP
mTOR
FOXO1
TXNIP
ROS
Caspase3/7
NLRP3 inflammasome
IL-1β
IL-1β
IL-1β
IL-1β
pro-Caspase-1
Caspase-1
pro-IL-1β
IL-1β
③ ④
IL-1β
③
IL-1β
④
The first hit
The second hit